Computation of turbulent natural convection at vertical walls using new wall functions

M. Hölling, H. Herwig

Institute of Thermo-Fluid Dynamics
Hamburg University of Technology
Denickestraße 17, 21073 Hamburg, Germany
m.hoelling@tu-harburg.de
h.herwig@tu-harburg.de

1. Introduction

Natural convection can be observed in technical applications, e.g. climatisation of buildings or cooling of electronic devices, as well as in nature, e.g. oceanic or atmospheric flows. In this study, turbulent natural convection at heated or cooled walls is analysed asymptocically. Often, natural convection is studied at simple geometries as shown in Figure 1. A 1-D situation is encountered in an infinite vertical channel, see Versteegh and Nieuwstadt [1] as well as Betts and Bokhari [2], for example. Natural convection along a vertical plate was investigated by Tsuji and Nagano [3, 4] among others. Ampofo and Karayanis [5] conducted experiments for a low aspect ratio cavity with side walls at different temperatures.

All cases can be characterised by a Grashof number based on the channel width h or the distance along the plate, L

$$\mathrm{Gr} = \frac{g_x \beta \Delta T h^3}{\nu^2} \qquad \text{or} \qquad \mathrm{Gr}_L = \frac{g_x \beta \Delta T L^3}{\nu^2}. \tag{1}$$

In the near wall region, the governing equations for turbulent natural convection reduce to

$$0 = \frac{\partial}{\partial y}\left(a\frac{\partial T}{\partial y} - \overline{v'T'} \right) \tag{2}$$

$$0 = \frac{\partial}{\partial y}\left(\nu\frac{\partial u}{\partial y} - \overline{u'v'} \right) + g_x\beta\,(T - T_0) \tag{3}$$

see for example Tsuji and Nagano [3].

A classical asymptotic theory was published by George and Capp [6] in which power laws for the temperature and velocity profiles are proposed. It is widely used, although Versteegh

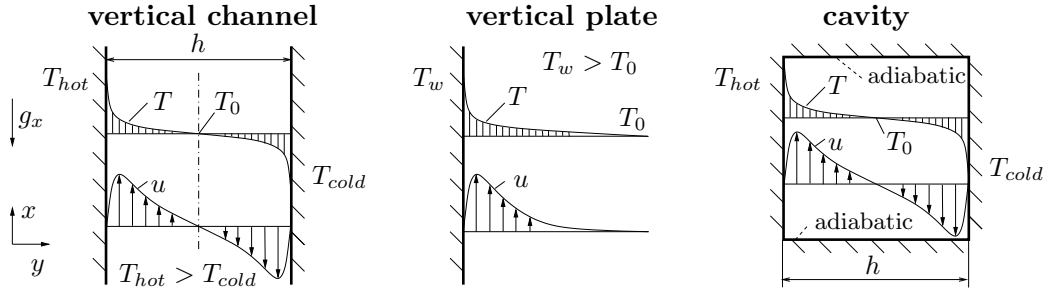

Figure 1: Standard geometries for turbulent natural convection. Left: infinite vertical channel [1, 2]; Middle: vertical plate [3, 4]; Right: cavity with differentially heated sidewalls [5]

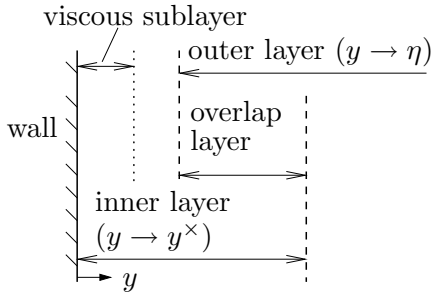

Figure 2: Two-layer-structure of the temperature field for turbulent natural convection

and Nieuwstadt [1] and Henkes and Hoogendorn [7] showed deviations between this theory and their data. An alternative approach was proposed by Yuan *et al.* [8], with profiles obtained by dimensional considerations and curve fitting.

Despite the intensive research in natural convection for the last decades there is no theory available today that can accurately describe the near wall region of natural convection. Therefore, we want to present new results, first shown in Hölling and Herwig [9] together with their implementation as wall functions in a CFD code. Results shown afterwards are valid for fluids with $\mathrm{Pr} = 0.7$.

2. Temperature Profiles

An expection of the energy equation, (2), shows that the heat flux consists of a molecular part ($a\,\partial T/\partial y$) and a turbulent part ($-\overline{v'T'}$) with its sum equal to the wall heat flux ($a\,\partial T/\partial y|_w$). Thus, the wall heat flux can be identified as the crucial parameter in turbulent natural convection and a characteristic temperature T_c should be based on it. Following dimensional considerations we introduce

$$T_c \equiv \left(\frac{a^2}{g\beta} \left.\frac{\partial T}{\partial y}\right|_w^3 \right)^{1/4} \qquad \text{and} \qquad \Theta^\times \equiv \frac{T_w - T}{T_c} \tag{4}$$

as the non-dimensional temperature $\Theta^\times$.

Next, the wall distance has to be non-dimensionalised. Analysing the temperature field, it turns out that it has a two-layer-structure as shown in Figure 2. Close to the wall an *inner layer* exists in which molecular and turbulent heat transfer are present. The region further away from the wall is identified as the *outer layer* which is dominated by turbulent heat transfer.

For $\mathrm{Gr} \to \infty$ the ratio of these two layers tends to zero leading to a singular temperature profile at the wall. Thus, two different non-dimensional wall distances have to be introduced, one for the inner and one for the outer layer. The thickness δ of the inner layer scales as

$$\delta = T_c \left.\frac{\partial T}{\partial y}\right|_w^{-1} \tag{5}$$

and the non-dimensional wall distance for the inner layer is $y^\times \equiv y/\delta$. For the outer layer a geometric length (channel width h or distance along the plate L) can be used as a length scale, resulting in $\eta \equiv y/h$ (or $\eta \equiv y/L$).

As shown in Figure 2 the two layers are not sharply separated but an *overlap layer* exists in-between. In this overlap layer, the temperature field can be simultaneously described in terms of the inner layer (using $y^\times$) and the outer layer (using η). An asymptotic matching of gradients in this layer results in

$$\lim_{y^\times \to \infty} y^\times \frac{\partial \Theta^\times}{\partial y^\times} = \lim_{\eta \to 0} \eta \frac{\partial \Theta^\times}{\partial \eta}. \tag{6}$$

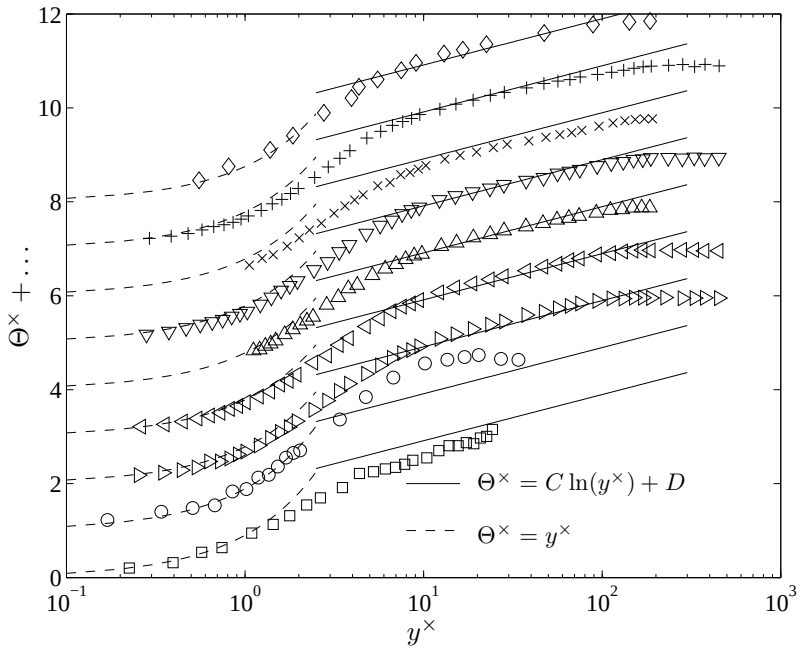

Figure 3: Non-dimensional temperature profiles of Betts and Bokhari [2] for Gr = 1.43 10^6 (□), from Ampofo and Karayiannis [5] for Gr = 1.59 10^9 (○), of Tsuji and Nagano [3] for $\mathrm{Gr}_L = 1.55\ 10^{10}$ (▷), for $\mathrm{Gr}_L = 3.62\ 10^{10}$ (◁), for $\mathrm{Gr}_L = 7.99\ 10^{10}$ (△), for $\mathrm{Gr}_L = 8.44\ 10^{10}$ (▽), for $\mathrm{Gr}_L = 8.99\ 10^{10}$ (×), for $\mathrm{Gr}_L = 17.97\ 10^{10}$ (+) and of Cheesewright [10] for $\mathrm{Gr}_L = 8.65\ 10^{10}$ (◇). Profiles are shifted by one unit each for better clarity.

This equation can only be fulfilled if both sides are equal to a constant C. Integration of equation (6) therefore leads to

$$\Theta^\times = C \ln\left(y^\times\right) + D. \tag{7}$$

The constants $C = 0.427$ and $D = 1.93$ were determined by comparison with experimental and numerical data. Figure 3 shows temperature profiles from various studies in their non-dimensional form. The agreement between the data and the logarithmic profile according to equation (7) is quite good. Additionally the temperature profile for the viscous sublayer is plotted. In this region adjacent to the wall heat transport is purely molecular (see Figure 2) and the temperature profiles are $\Theta^\times = y^\times$, following from equation (2). This again is in good agreement with the data.

Here, as well as for the velocity profiles in the next section, variable property effects had to be taken into account when constants were determined from experimental data, see Hölling and Herwig [9] for details.

3. Velocity Profiles

In a straightforward approach, as applied by George and Capp [6], velocity gradients are matched in the overlap layer. This, however, results in a poor representation of the flow field [1, 7]. Instead, in our study the velocity profile in the overlap layer is directly derived from the momentum equation (3). With an eddy-viscosity approach, $-\overline{u'v'} = \nu_t\, \partial u/\partial y$, together with $\nu_t \gg \nu$ equation (3) in non-dimensional form reads

$$0 = \frac{\partial}{\partial y^\times}\left(\frac{\nu_t}{\nu}\,\frac{\partial U^\times}{\partial y^\times}\right) - \Theta^\times + \Theta_0^\times \tag{8}$$

with $U^\times = u/u_c$ as non-dimensional velocity based on

$$u_c = \frac{g_x \beta T_c^3}{\nu} \left| \frac{\partial T}{\partial y} \right|_w^{-2}. \tag{9}$$

$U^\times$ can be obtained by integrating equation (8) with all terms rewritten as functions of $y^\times$. Since the temperature profile is already known in terms of $y^\times$, see (7), only $\nu_t/\nu = f(y^\times)$ has to be found. First, this expression is rewritten with the turbulent Prandtl number σ_t as

$$\frac{\nu_t}{\nu} = \frac{\sigma_t}{\mathrm{Pr}} \frac{a_t}{a}. \tag{10}$$

From the DNS data of Versteegh and Nieuwstadt [1] it is found that σ_t is nearly constant in the overlap layer with $\sigma_t = 0.9$, like for forced convection. The ratio of the turbulent thermal diffusivity a_t and the molecular thermal diffusivity a can be obtained by differentiating the temperature profile (7) and comparing it to the non-dimensional form of equation (2). From this

$$\frac{a_t}{a} = \frac{y^\times}{C} \qquad \Rightarrow \qquad \frac{\nu_t}{\nu} = \frac{\sigma_t}{\mathrm{Pr}} \frac{y^\times}{C}. \tag{11}$$

Now, all terms in equation (8) depend on $y^\times$ only and it can be integrated, from which

$$U^\times = \frac{C\mathrm{Pr}}{\sigma_t} y^\times \left(C \left[\ln(y^\times) - 2 \right] + D - \Theta_0^\times \right) + E \ln(y^\times) + F \tag{12}$$

results. The "constants" of integration, E and F, are constant with respect to $y^\times$ but they depend on the non-dimensional wall shear stress $\partial U^\times/\partial y^\times|_w$:

$$E = 0.49 \left. \frac{\partial U^\times}{\partial y^\times} \right|_w - 2.27 \qquad \text{and} \qquad F = 1.28 \left. \frac{\partial U^\times}{\partial y^\times} \right|_w + 1.28 \tag{13}$$

This was found by comparison with numerical and experimental data.

Figure 4 shows non-dimensional velocity profiles from various studies. The velocity profiles in the overlap layer, equation (12), are a good representation (better than the profiles from George and Capp [6]) of the experimental data as long as the Grashof number is high enough. Additionally, the velocity profiles in the viscous sublayer are shown, obtained by integrating equation (3) with $-\overline{u'v'} = 0$. In its non-dimensional form they read

$$U^\times = \frac{1}{6} y^{\times 3} - \frac{1}{2} \Theta_0^\times y^{\times 2} + \left. \frac{\partial U^\times}{\partial y^\times} \right|_w y^\times. \tag{14}$$

Equation (14) again is a good representation of the experimental data.

The temperature and velocity profiles, (7) and (12), respectively, are valid for equilibrium boundary layers and for wall angles α (angle between the wall and a horizontal line) with $30° \lesssim \alpha < 90°$. For $\alpha \neq 90°$ only the component of the gravitational acceleration parallel to the wall has to be taken into account ($g_x = g \sin\alpha$). For $\alpha \approx 0°$ (Rayleigh-Bénard convection) alternative temperature and velocity profiles can be derived, see e.g. Hölling and Herwig [11, 12].

4. Implementation in CFD codes

The temperature and velocity profiles derived above can be used as *wall functions* for natural convection in CFD codes, so that coarse grids can be used near the wall. Then, the flow and temperature fields are not resolved up to the wall, but the center of the first control volume lies within the overlap layer. The region close to the wall is brigded by the wall functions, i.e. gradients at the wall are determined using the universal profiles (7) and (12).

First, results for natural convection from a commercial CFD-code are shown to emphasize the need for a new wall treatment. In the subsequent section results are given that were obtained with the new wall functions.

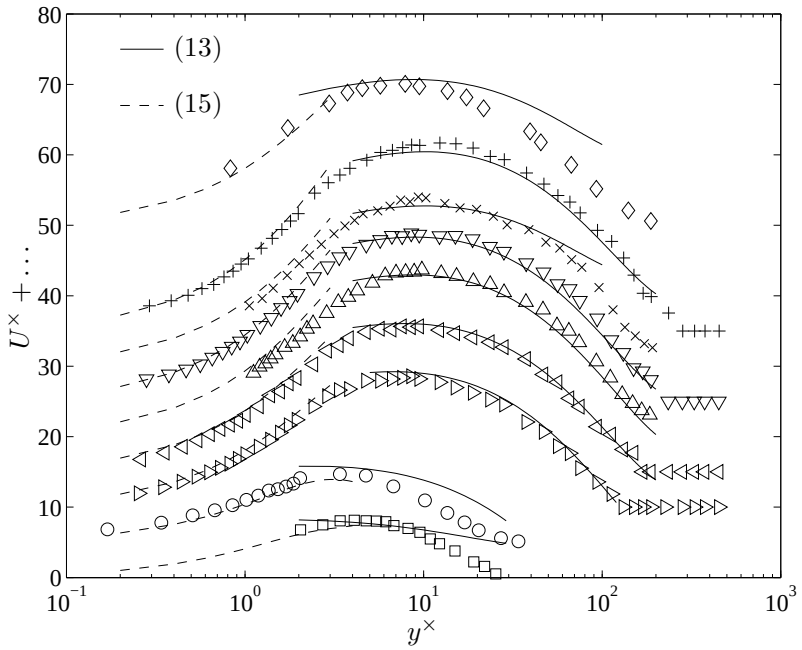

Figure 4: Non-dimensional velocity profiles of Betts and Bokhari [2] for Gr = 1.43 10^6 (□), from Ampofo and Karayiannis [5] for Gr = 1.59 10^9 (○), of Tsuji and Nagano [3] for Gr_L = 1.55 10^{10} (▷), for Gr_L = 3.62 10^{10} (◁), for Gr_L = 7.99 10^{10} (△), for Gr_L = 8.44 10^{10} (▽), for Gr_L = 8.99 10^{10} (×), for Gr_L = 17.97 10^{10} (+) and of Cheesewright [10] for Gr_L = 8.65 10^{10} (◇). Profiles are shifted by five units each for better clarity.

4.1 Commercial Code Results

FLUENT 6.2 was chosen to test the performance of a state-of-the-art commercial CFD-code for turbulent natural convection. The DNS results of Versteegh and Nieuwstadt [1] served as a benchmark case. The geometry is a heated vertical infinite channel (see Figure 1, left) with $\mathrm{Ra} = \mathrm{Gr}\,\mathrm{Pr} = 5.0\,10^6$ and Pr = 0.7. Two different grid sizes were used, i.e. a coarse grid with FLUENT standard wall treatment and a fine grid resolving the viscous sublayer ($y^+ \approx 1$). Additionally, four different (two-equation) turbulence models were tested on both grids.

Wall gradients were chosen to assess the performance of various combinations since they are equivalent to the wall heat flux and wall shear stress, both important quantities. In the numerical results temperature wall gradients deviate by $20 \div 40\%$, velocity wall gradients by $20 \div 70\%$. Best results were obtained with the k-ω turbulence model for which the corresponding profiles are shown in Figure 5. In view of the errors in temperature and velocity gradients and deviations especially in the velocity profiles it can be concluded that commercial codes with standard turbulence modeling and wall treatment give only poor results for turbulent natural convection.

4.2 New Wall Functions

In order to improve the insufficient results of standard models for turbulent natural convection our new wall functions were implemented in the OpenSource CFD-code CAFFA [13] with the k-ω turbulence model and the Boussinesq approximation to account for buoyancy effects. By means of equation (7) and (12) wall gradients for the temperature and velocity are calculated, respectively. For simplicity, the boundary condition for k (turbulent kinetic energy) is $k = u_\tau^2/0.3$, like in forced convection. The boundary condition for ω (dissipation rate), however, was

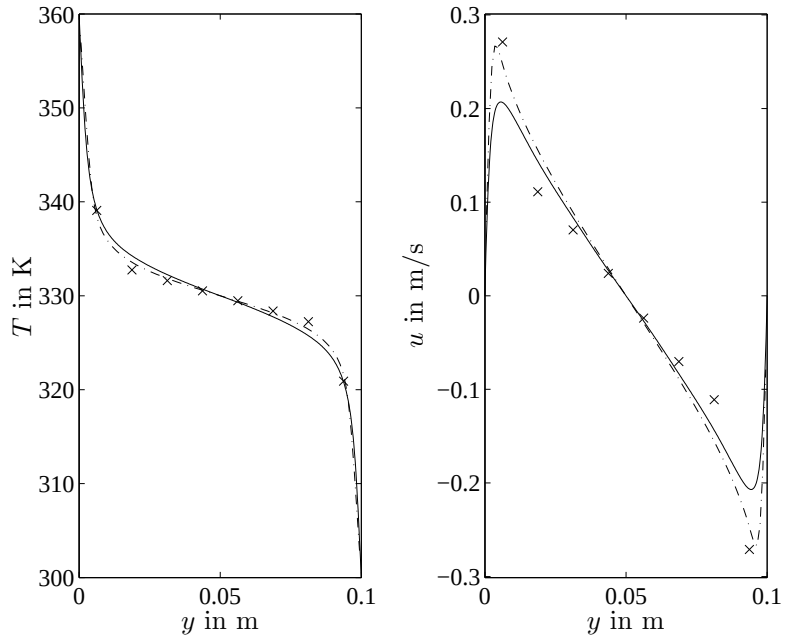

Figure 5: FLUENT results ($- \cdot -$: fine grid; $\times$: coarse grid) with the k-ω turbulence model compared to the DNS data of Versteegh and Nieuwstadt [1] for $\mathrm{Ra} = \mathrm{Gr}\,\mathrm{Pr} = 5.0\ 10^6$ (—).

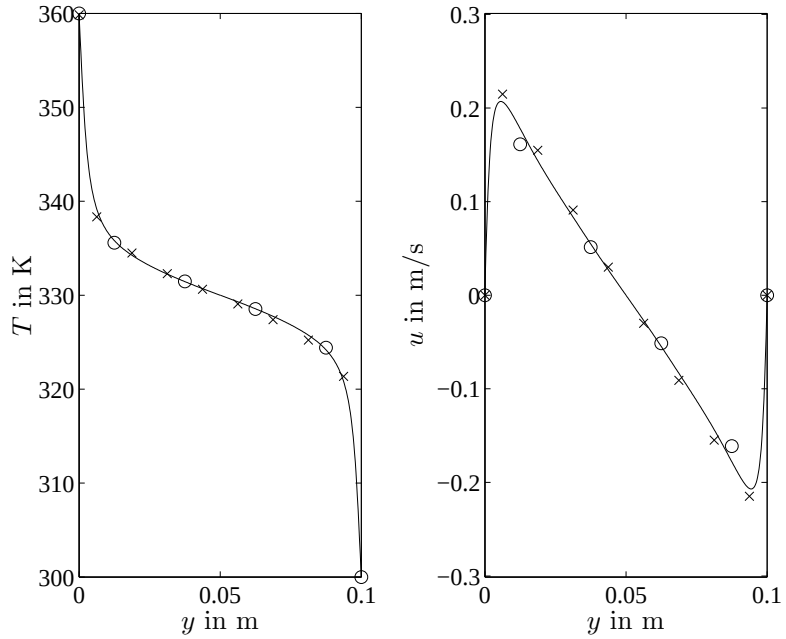

Figure 6: CAFFA results ($\times$: eight cells; $\circ$: four cells) using new wall functions compared to the DNS data of Versteegh and Nieuwstadt [1] for $\mathrm{Ra} = \mathrm{Gr}\,\mathrm{Pr} = 5.0\ 10^6$ (—).

modified. Taking advantage of $\nu_t = k/\omega$ and

$$\nu_t = \nu \frac{\sigma_t}{\mathrm{Pr}} \frac{y^\times}{C}, \tag{15}$$

according to equation (11), the boundary condition for ω is

$$\omega = \frac{k}{\nu} \frac{\mathrm{Pr}}{\sigma_t} \frac{C}{y^\times}. \tag{16}$$

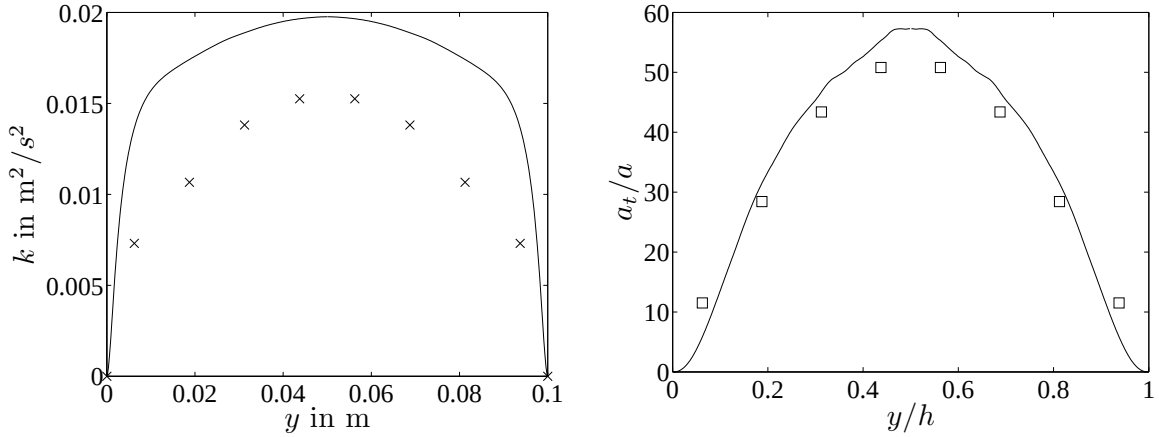

Figure 7: CAFFA results for the turbulent kinetic energy k ($\times$, left) and the ratio of turbulent and molecular thermal diffusivity, a_t/a, ($\square$, right) compared to the DNS data of Versteegh and Nieuwstadt [1] for $\mathrm{Ra} = 5.0\,10^6$ (—).

The proposed set of wall functions / boundary conditions can be used when the center of the first control volume is within the overlap layer ($y^\times \gtrsim 5$).

In Figure 6 results for the infinite vertical channel ($\mathrm{Ra} = 5.0\,10^6$) obtained with the new wall functions and modified turbulence boundary conditions are shown. Deviations of the wall gradients with respect to DNS results are within 3 % compared to $20 \div 70$ % of the FLUENT results. Also, the computation time can be reduced considerably due to the coarse grids that can now be used. Figure 7 shows the profile of turbulent kinetic energy k and the ratio of turbulent and molecular thermal diffusivities, a_t/a, compared to the DNS data [1]. Though k deviates from the DNS data, a_t/a is quite close to the data in [1]. This is due to the modified boundary condition for ω, equation (16), by which the correct value of ν_t (and therefore also a_t) in the control volume adjacent to the wall is enforced.

The good agreement of the mean flow field and the rather poor representation of k and ω are not unique for natural convection but can also be observed in forced convection. Numerical solutions for complex interior forced convection flows, as measured by Mocikat *et al.* [14], for example, show good agreement for the mean flow profiles based on standard CFD code results. However, e.g. the turbulent kinetic energy k then is wrong by more than 100 %.

The proposed set of wall functions / boundary conditions together with a standard turbulence model may be a reasonable approach as long as there is no better turbulence model for natural convection.

5. Conclusions

The temperature and velocity profiles for turbulent natural convection at vertical walls were analysed asymptotically. A two-layer structure can be identified with a viscosity influenced inner layer and a turbulent outer layer. The temperature profile is obtained by asymptotic matching of temperature gradients in the overlap layer. The momentum equation is rewritten in terms of the wall distance and can then be integrated to get the velocity profile for the overlap layer. These profiles, (7) and (12), are in good agreement with numerical and experimental data sets.

These profiles can be used in CFD-codes as improved wall functions for natural convection since commercial codes with standard wall treatment give only poor results. The standard k-ω turbulence model was chosen with a modified boundary condition for ω. Results for the

temperature and velocity profiles are in good agreement with DNS data, though the profile for the turbulent kinetic energy k show considerable deviations.

An alternative turbulence model adapted to natural convection is needed to improve the agreement for k (and ω). Also, an extension to mixed convection at vertical walls is planned, see for example Balaji *et al.* [15]. Additionally, an extension to non-equilibrium boundary layers would be an option to increase the range of validity.

References

[1] T.A.M. Versteegh and F.T.M. Nieuwstadt, "A direct numerical simulation of natural convection between two infinite vertical differentially heated walls: scaling laws and wall functions", *Int. J. Heat Mass Transfer* **42**, 3673–3693 (1999).

[2] P.L. Betts and I.H. Bokhari, "Experiments on turbulent natural convection in an enclosed tall cavity", *Int. J. Heat Fluid Flow* **21**, 675–683 (2000).

[3] T. Tsuji and Y. Nagano, "Characteristics of a turbulent natural convection boundary layer along a vertical flat plate", *Int. J. Heat Mass Transfer* **31**, 1723–1734 (1988).

[4] T. Tsuji and Y. Nagano, "Turbulence measurements in a natural convection boundary layer along a vertical flat plate", *Int. J. Heat Mass Transfer* **31**, 2101–2111 (1988).

[5] F. Ampofo and T.G. Karayiannis, "Experimental benchmark data for turbulent natural convection in an air filled square cavity", *Int. J. Heat Mass Transfer* **46**, 3551–3572 (2003).

[6] W.K. George and S.P. Capp, "A theory for natural convection turbulent boundary layers next to heated vertical surfaces", *Int. J. Heat Mass Transfer* **22**, 813–826 (1979).

[7] R.A.W.M. Henkes and C.J. Hoogendoorn, "Numerical determination of wall functions for the turbulent natural convection boundary layer", *Int. J. Heat Mass Transfer* **33**, 1087–1097 (1990).

[8] X. Yuan, A. Moser and P. Suter, "Wall functions for numerical simulation of turbulent natural convection along vertical plates", *Int. J. Heat Mass Transfer* **36**, 4477–4486 (1993).

[9] M. Hölling and H. Herwig, "Asymptotic analysis of the near wall region of turbulent natural convection flows", *J. Fluid Mech.* **541**, 383–397 (2005).

[10] R. Cheesewright, "Turbulent natural convection from a vertical plane surface", *J. Heat Transfer* **90**, 1–8 (1968).

[11] M. Hölling and H. Herwig, "A new Nusselt/Rayleigh number correlation and wall functions for turbulent Rayleigh-Bénard convection", *Proc. IHTC13* Sydney, 13.-18. August, (2006).

[12] M. Hölling and H. Herwig, "Asymptotic analysis of heat transfer in turbulent Rayleigh-Bénard convection", *Int. J. Heat Mass Transfer* , **49**, 1129–1136 (2006).

[13] J.H. Ferziger and M. Peric, "Computational methods for fluid dynamics", *2nd ed., Springer, Berlin* (1999).

[14] H. Mocikat, T. Gürtler and H. Herwig, "Laser Doppler velocimetry measurements in an interior flow test facility: A database for CFD-code evaluation", *Exp. in Fluids* **34**, 442–448 (2003).

[15] C. Balaji, M. Hölling and H. Herwig, "New approaches to treatment of turbulent mixed convection flows using asymptotics", *submitted for publication* (2006).